



**HAL**  
open science

## Doubling of the phase transition temperature of VO<sub>2</sub> by Fe doping

Jean-Louis Victor, Manuel Gaudon, Giorgio Salvatori, Olivier Toulemonde,  
Nicolas Penin, Aline Rougier

► **To cite this version:**

Jean-Louis Victor, Manuel Gaudon, Giorgio Salvatori, Olivier Toulemonde, Nicolas Penin, et al.. Doubling of the phase transition temperature of VO<sub>2</sub> by Fe doping. *Journal of Physical Chemistry Letters*, 2021, 12 (32), pp.7792-7796. 10.1021/acs.jpcclett.1c02179 . hal-03326220

**HAL Id: hal-03326220**

**<https://hal.science/hal-03326220>**

Submitted on 25 Aug 2021

**HAL** is a multi-disciplinary open access archive for the deposit and dissemination of scientific research documents, whether they are published or not. The documents may come from teaching and research institutions in France or abroad, or from public or private research centers.

L'archive ouverte pluridisciplinaire **HAL**, est destinée au dépôt et à la diffusion de documents scientifiques de niveau recherche, publiés ou non, émanant des établissements d'enseignement et de recherche français ou étrangers, des laboratoires publics ou privés.

# Doubling of the phase transition temperature of VO<sub>2</sub> by Fe doping

Jean-Louis Victor, Manuel Gaudon, Giorgio Salvatori, Olivier Toulemonde, Nicolas Penin,  
and Aline Rougier

CNRS, Univ. Bordeaux, Bordeaux INP, ICMCB (UMR 5026), Pessac F-33600, France

**ABSTRACT:** Vanadium dioxide (VO<sub>2</sub>) undergoes a fully reversible first order metal–insulator transition (MIT) from M1 monoclinic phase (*P2<sub>1</sub>/c*) to a high-temperature tetragonal phase (*P4<sub>2</sub>/mmm*) at around 68 °C. Modulate phase transition of VO<sub>2</sub> by chemical doping is becoming of fundamental and technological interest. Here, we report the synthesis of highly-crystallized Fe-doped VO<sub>2</sub> powders by a carbo-thermal reduction process. The impact of Fe doping on structural and phase transition of VO<sub>2</sub> is studied. The as-prepared Fe-doped VO<sub>2</sub> samples crystallize in M2 monoclinic form (*C2/m*), which could be due to a segregation of the doping ions in the V2 zig-zag chains. A strong increase of the transition temperature up to 134 °C is observed, which does represent a breakthrough in the VO<sub>2</sub>-type thermochromic materials.

Vanadium dioxide (VO<sub>2</sub>) is a well-known thermochromic material, which undergoes a fully reversible first order metal–insulator transition (MIT) from a low-temperature monoclinic M1 phase (*P2<sub>1</sub>/c*) to a high-temperature tetragonal phase (*P4<sub>2</sub>/mmm*) at around 68 °C. At the MIT, significant changes of atomic organisation are intertwined with changes of the electrical, the optical, and the magnetic properties<sup>1-2</sup>, making VO<sub>2</sub> a promising candidate for switching applications<sup>3-4</sup>, but with remaining controversies about the Peierls or Mott origin for the phase transition<sup>5-11</sup>. In our own previous studies, considering that the phase transition is well linked to structural origin, geometrical calculations in agreement with experimental studies suggested that VO<sub>2</sub> phase transition is the consequence of very short atomic shifts mainly associated to a decrease of the 2nd sphere coulombic interactions<sup>12</sup>. For practical use, various transition temperatures of VO<sub>2</sub> are desired to fulfil the different demands depending on the applications. For illustration, a transition temperature (T<sub>MIT</sub>) around 30°C is suitable for thermochromic smart windows<sup>13</sup>, whereas T<sub>MIT</sub> above 110°C is required for solar thermal collector optimization<sup>14-15</sup>. Great efforts have been devoted toward accomplishing modulation of T<sub>MIT</sub> and doping is the most widespread and efficient approach to achieve this objective. Relying on a Mott-driven transition mechanism, high-valence dopants act as free electrons donors into the VO<sub>2</sub> conduction band and lower the T<sub>MIT</sub><sup>16</sup>, while substitution of V<sup>4+</sup> by ions with lower valence such as Fe<sup>3+</sup>, Al<sup>3+</sup> or Cr<sup>3+</sup> stabilize the intermediate phase M2 and slightly raise T<sub>MIT</sub><sup>17-19</sup>. W<sup>6+</sup> has been considered as one of the most effective donor-like dopant, lowering the transition temperature by 24°C per 1 mol%<sup>20</sup>. On the other side, as far as we know, the highest T<sub>MIT</sub> is demonstrated at ~105°C for 10 mol% Cr-doped VO<sub>2</sub><sup>21</sup>.

Fe-doped VO<sub>2</sub> has already been studied<sup>17,22,23,24,25</sup>, but the effect of Fe dopant on the MIT transition remains misunderstood. So far, the studies reveal that Fe doping does not really affect the MIT transition of VO<sub>2</sub>.

In the current work, we report the synthesis and characterization of highly-crystallized Fe-doped VO<sub>2</sub> powders. The evaluation of the impact of Fe doping on the MIT transition is the main target. A pyrolysis method was used to synthesize Fe-doped VO<sub>2</sub> powder with Fe content up to 12.6 mol%. In a first stage, iron acetate (FeOH(CH<sub>3</sub>COO)<sub>2</sub>) and NH<sub>4</sub>VO<sub>3</sub> precursors were dissolved in excess ethylene glycol (C<sub>2</sub>H<sub>6</sub>O<sub>2</sub>, 80 mL) and refluxed in an oil bath at 160°C for two hours to produce Fe-doped vanadyl ethylene glycolate (Fe-VEG). The Fe-VEG powder was then annealed under air atmosphere at 300°C for 3 hours to obtain Fe-doped nano-V<sub>2</sub>O<sub>5</sub>. Finally, the Fe-doped V<sub>2</sub>O<sub>5</sub> powder was mixed with carbon and annealed in a flowing Ar atmosphere at 800 °C for 15 hours to obtain pure Fe-doped VO<sub>2</sub>. The Fe content in each Fe-doped VO<sub>2</sub> powder was carefully determined by inductively coupled plasma (ICP) analysis. Three different doping percentages were obtained: 5.5%, 9.0% and 12.6%. The crystal structure, the morphology and the phase transition properties of the synthesized powders were investigated by X-ray diffraction (XRD), scanning electron microscopy (SEM) and differential scanning calorimetry (DSC), respectively.

Figure 1 shows XRD patterns of 0%, 5.5%, 9.0% and 12.6% Fe-doped VO<sub>2</sub> samples. For the undoped VO<sub>2</sub> powder, all the room-temperature X-ray peaks match with the monoclinic (*P2<sub>1</sub>/c*) M1 VO<sub>2</sub> (JCPDS 44-0252). The XRD patterns for all Fe-doped VO<sub>2</sub> samples are quite similar and do not belong to the monoclinic M1 VO<sub>2</sub>, indicating the formation of a new structural symmetry induced by Fe-doping. The twin peaks around 2θ = 27.3° and 28.5° for the Fe-doped samples (Figure 1b) are assigned to (-201) and (201) planes of the monoclinic (*C2/m*) M2 VO<sub>2</sub>. It's interesting to note that the obtained M2 phase reveals less peaks than expected. Indeed, peaks around 2θ = 26.5°, 2θ = 34.0°, 2θ = 48.0° and 2θ = 53.0° are missing compared to M2 phase already reported in the literature<sup>18</sup>. A higher-symmetric structure could explain such structural properties. In addition, the (-201) diffraction peaks significantly shift toward the low-angle region promoting a gap between (-201) and (201) planes with increasing Fe-doping amount, pointing out an expansion of the VO<sub>2</sub> unit-cell. This indirectly indicates that the larger Fe<sup>3+</sup> ions (0.645 Å compared to 0.58 Å for V<sup>4+</sup>) are successfully incorporated into the VO<sub>2</sub> lattice. Low intensity extra peaks are observed for the 12.6 mol% Fe-doped sample corresponding to Fe<sub>2</sub>O<sub>3</sub> phase<sup>26</sup>, which means that the solubility limit of Fe in VO<sub>2</sub> is reached.

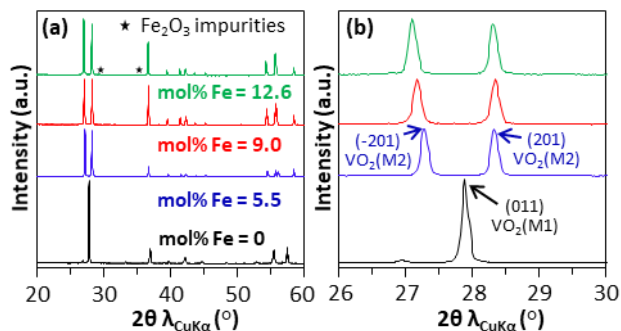


**Figure 1.** Room temperature XRD patterns of Fe-doped VO<sub>2</sub> powders with different Fe-doping concentrations (a) and focus on the 26 to 30° 2θ region (b).

It is well-known that the first order phase transition of VO<sub>2</sub> is associated with a large variation of latent heat, quantifiable by thermal analysis. The DSC analysis of the Fe-doped VO<sub>2</sub> powders was performed using the same scanning conditions (temperature range: 30-160°C, rate: 10°C/min, atmosphere: N<sub>2</sub>). To test the repeatability and to detect the potential switching fatigue, each sample was subjected to three measurement cycles. The DSC curves are displayed in Figure 2. The similarity of the successive DSC curves throughout the 3 cycles for all samples illustrates the non-fatigability of the MIT. By convention, the T<sub>MIT</sub> is taken as the average of endothermic and exothermic peak positions. A drastic shift of the T<sub>MIT</sub> toward higher values is observed as the doping content increases, especially between the 5.5 and 9.0% Fe-doped samples. This trend well agrees with previous studies in which transition temperature was observed to change significantly only for relative dopant concentrations exceeding 6 mol%<sup>21,27</sup>. The transition temperature finally increases up to 133.4°C for the 12.6% Fe-doped VO<sub>2</sub> sample, which is twice higher than the original value. This result is far better than what can be found in the literature for Fe-doped VO<sub>2</sub> or even any other metal-doped VO<sub>2</sub><sup>17,18,28</sup>. Also, the higher T<sub>MIT</sub> value reported so far is around 105 °C for Cr-doped VO<sub>2</sub><sup>21</sup>. The huge impact of dopant on T<sub>MIT</sub> may be related to the synthesis process, which allows a high dopant concentration in the VO<sub>2</sub> phase to be achieved. Nevertheless, the DSC peaks in Fe-doped samples get broader and weaker compared with those of undoped sample. The increment of defect states caused by the dopant ions could explained this phenomenon. The 9.0 mol% Fe-doped VO<sub>2</sub> sample reveals very interesting thermochromic properties (T<sub>MIT</sub> around 118 °C) without Fe<sub>2</sub>O<sub>3</sub> impurities. This sample was chosen to be further characterized.

SEM image of the 9.0 mol% Fe-doped VO<sub>2</sub> powder is shown in Figure 3 and reveals micrometer size crystallites with clearly faceted surfaces. The chemical composition of different crystallites was also determined from dispersive X-ray (EDX) using a spot size equal to 3 x 3 μm<sup>2</sup>. Measurements were performed on five isolated grains and the Fe/V molar ratio was calculated from the Kα peak of each element. The doping level within individual grains is found to be uniform with a Fe content in the narrow range: 8.8-9.5%, in good agreement with the average value of 9.0% obtained by ICP analysis. Thus, the synthesis process allows the obtaining of very large particles size with a homogeneous distribution of the Fe dopant.

Rietveld refinement method was thereafter conducted to determine the crystal structure of the 9.0 mol% Fe-doped VO<sub>2</sub>. A crystal structure model was firstly built from the M2 crystal description previously reported in literature, i.e. considering two kinds of V-V chains: zigzag chains with equidistant V-V bonds (V2 atoms), and linear chains with alternatively short and long V-V bonds (V1 atoms) (Figure 4a).

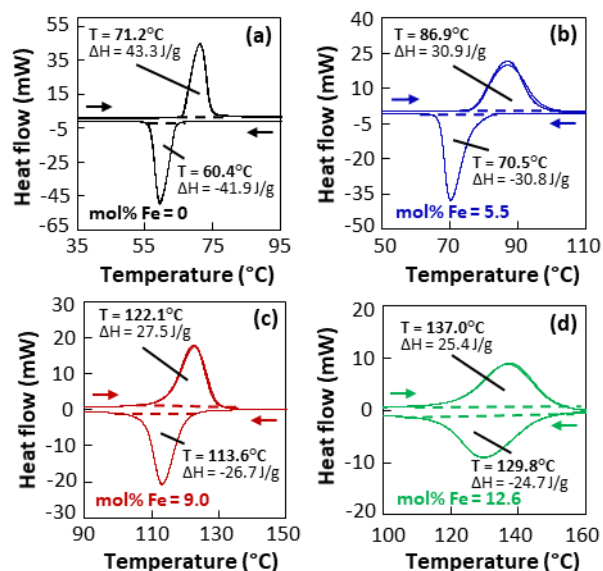


**Figure 2.** DSC curves of 0 mol% (a) 5.5 mol% (b) 9.0 mol% (c) and 12.6 mol% (d) Fe-doped VO<sub>2</sub> samples.

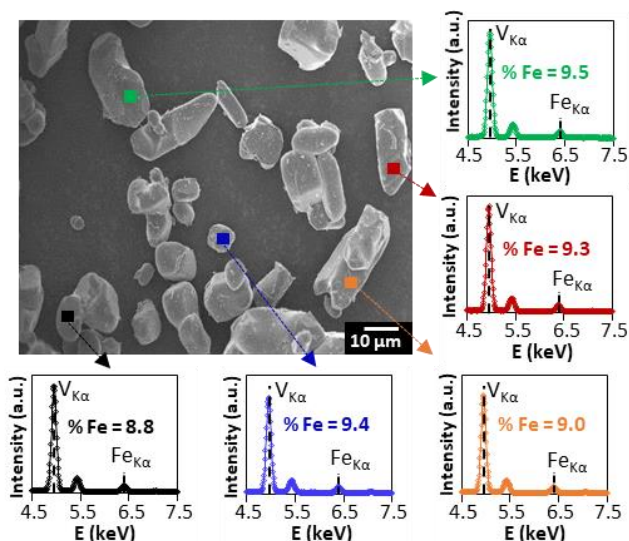


**Figure 3.** SEM image and the EDX spectra of 9.0 mol% Fe-doped VO<sub>2</sub> sample (spot size for EDX analysis: 3 x 3 μm<sup>2</sup>).

In comparison with the standard pure VO<sub>2</sub> M1 phase, which exhibits a single zig-zag chain within V-V pairing configuration, M2 phase crystallographic network exhibits a discrimination in two V-V chains, with for both channels, an exaltation of one of the configurational parameters (zig-zag or V-V pairing), and an extinction of the other. It can be noted that peak intensities are not correctly taken into account considering such crystal structure, explaining the agreement factors are quite high. Also, the very large isotropic displacement factor calculated for the V2 atom suggests a segregation of the Fe defects located on the zigzag chains and Fe was so introduced on a secondary position in this first chain in a second refinement model. Finally, in a second round, the model was optimized also distinguishing two sub-positions for the V1 atoms (Figure 4b). The introduction of Fe in V2 chains with a refined occupancy (7 mol%) in quite good agreement with experimental doping concentration, as well as the 50-50 distribution of the V1 atoms in their two sub-positions showing a degree of freedom of the antiferroelastic pairing in V1 chains respectively to the zig-zag V2 chains orientation, lead to a significantly better X-ray pattern refinement with a realistic struc-

tural model. The lattice parameters, the atomic positions and the agreement factors ( $R_{\text{Bragg}}$  and  $R_{\text{F}}$ ) obtained after Rietveld refinements are summarized in Table 1.

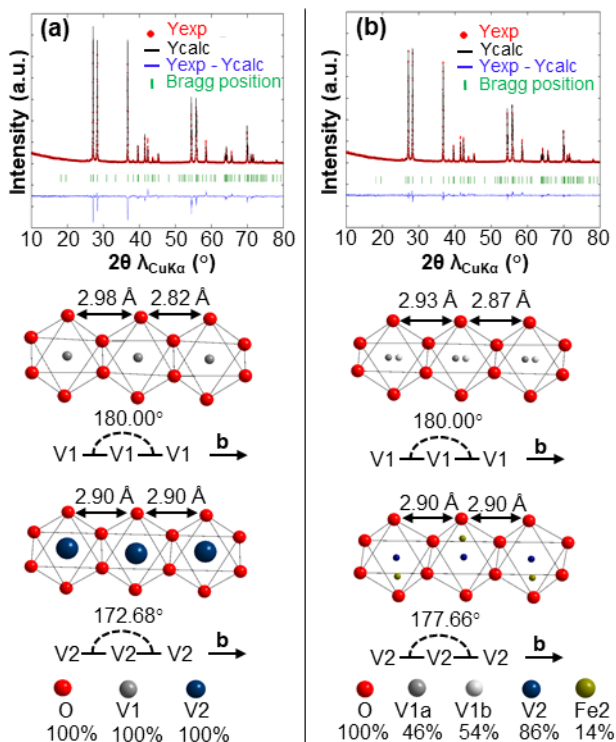


**Figure 4.** Rietveld refinement of 9 mol% Fe-doped VO<sub>2</sub> powder using a conventional M2 crystal structure model (a) and a new model distinguishing two sub-positions for the V1 atom and introducing Fe atom in V2 chains (b) (the size of each atom is correlated to the atomic isotropic displacement parameter  $B_{\text{iso}}$ , which may represent atomic motion and possible static displacive disorder).

**Table 1.** Structural parameters obtained after Rietveld refinement of 9 mol% Fe-doped VO<sub>2</sub>.

Structural parameters Fig.4a					
C 2/m	a = 9.110(1) Å	α = 90°	$R_{\text{Bragg}} = 21.2$		
	b = 5.799(1) Å	β = 92.369(1)°	$R_{\text{F}} = 14.0$		
	c = 4.555(1) Å	γ = 90°			
Atom	X	Y	Z	$B_{\text{iso}}$	occ
V1	0	0.251(1)	0	0.52(3)	0.5
V2	0.243(1)	0	0.514(2)	2.83(7)	0.5
O1	0.151(1)	0.243(4)	0.302(3)	1	1
O2	0.091(2)	0	0.773(4)	1	0.5
O3	0.092(2)	0.5	0.791(5)	1	0.5
Structural parameters Fig.4b					
C 2/m	a = 9.110(1) Å	α = 90°	$R_{\text{Bragg}} = 7.21$		
	b = 5.799(1) Å	β = 92.370(1)°	$R_{\text{F}} = 10.1$		
	c = 4.555(1) Å	γ = 90°			
Atom	X	Y	Z	$B_{\text{iso}}$	occ
V1a	0	0.291(1)	0	0.27(5)	0.23(1)
V1b	0	0.217(1)	0	0.27(5)	0.27(1)
Fe2	0.175(3)	0	0.665(6)	0.27(5)	0.07(1)
V2	0.248(1)	0	0.505(1)	0.27(5)	0.43(1)
O1	0.143(1)	0.253(1)	0.313(2)	1	1
O2	0.102(1)	0	0.834(2)	1	0.5
O3	0.108(1)	0.5	0.823(2)	1	0.5

To confirm DSC analyse, temperature-dependent XRD of the 9.0 mol% Fe-doped VO<sub>2</sub> sample was finally performed to study the phase transition during the heating (Figure 5). For  $T \leq 90^\circ\text{C}$ , the sample remains in the monoclinic M2 structure. When the temperature reaches 110°C, the tetragonal ( $P4_2/mnm$ ) VO<sub>2</sub>(R) structure emerges while the M2 peaks decrease in intensity, suggesting the beginning of the phase transition, which is consistent with the DSC analysis (Figure 2). Finally, for  $T = 130^\circ\text{C}$ , all the peaks match with the tetragonal VO<sub>2</sub>(R) structure, revealing that the transition from the M2 phase to R phase is completed.

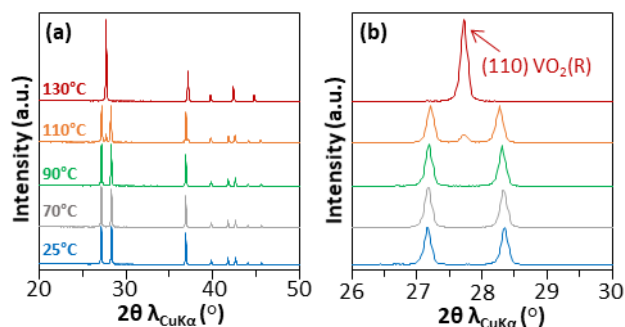


**Figure 5.** XRD patterns of the 9.0 mol% Fe-doped VO<sub>2</sub> sample collected at different temperatures during heating (a) and focus on the 26 to 30° 2θ region (b).

In conclusion, Fe-doped VO<sub>2</sub> powder was successfully synthesized at 800 °C in an Ar atmosphere for 15 hours from a carbo-thermal reduction process. All doped-samples are crystallized at room temperature in the monoclinic ( $C2/m$ ) M2 structure and DSC analysis revealed that Fe content strongly affect the MIT transition of VO<sub>2</sub>. The crystallization of the as-prepared Fe-doped VO<sub>2</sub> powders in the VO<sub>2</sub> (M2) form is to be linked with a segregation of the doping ions in the V2 zig-zag chains. This segregation, on a thermodynamic point of view, is related to lower over-potential of the Fe point defects in zig-zag chains than in linear one; one can note that, in our refinement model, the large Fe atoms out of centering from the geometrical centre of the octahedral site is surely closely related to this segregation. Consequently, with a Peierls concept view, Fe segregation in zigzag chains explains the M2 phase stabilization to the detriment of the M1 form and a re-investigation of the collected X-ray diffraction patterns using other doping elements is planned in the light of our proposal. Furthermore, the acclimatization of Fe-dopant in the accentuated zig-zag chains significantly stabilizes the M2 form to the detriment of the rutile symmetrical system and so increases the MIT phase transition temperature. A  $T_{\text{MIT}}$  of 134 °C has been reached with 12.6 mol% Fe, which represents a significant breakthrough in the inorganic thermochromic materials field. To the best of our knowledge, this is the highest transition temperature reported for doped VO<sub>2</sub>.

## AUTHOR INFORMATION

### Corresponding Author

**Manuel Gaudon** – CNRS, Univ. Bordeaux, Bordeaux INP, ICMCB (UMR 5026), Pessac F-33600, France  
Email: manuel.gaudon@icmcb.cnrs.fr

## ACKNOWLEDGMENT

The authors would like to thank Eric Lebraud and Sonia Buffiere for their assistance during XRD and SEM analysis.

## REFERENCES

- (1) Victor, J. L.; Marcel, C.; Sauques, L.; Penin, N.; Rougier, A. High quality thermochromic VO<sub>2</sub> thin films deposited at room temperature by balanced and unbalanced HiPIMS. *Solar Energy Materials & Solar Cells* **2021**, *227*, 111113-111121.
- (2) Guan, S.; Souquet-Basiège, M.; Toulemonde, O.; Denux, D.; Penin, N.; Gaudon, M.; Rougier, A. Toward Room-Temperature Thermochromism of VO<sub>2</sub> by Nb doping: Magnetic Investigations. *Chemistry of Materials* **2019**, *31*, 9819-9830.
- (3) Parrott, E. P. J.; Han, C.; Yan, F.; Humbert, G.; Bessadou, A.; Crunteanu, A.; Pickwell-MacPherson, E. Vanadium dioxide devices for terahertz wave modulation: a study of wire grid structures. *Nanotechnology* **2016**, *27*, 205206-205215.
- (4) Wang, H.; Yi, X.; Li, Y. Fabrication of VO<sub>2</sub> films with low transition temperature for optical switching applications. *Optics Communications* **2005**, *256*, 305-309.
- (5) Goodenough, J. The two components of the crystallographic transition in VO<sub>2</sub>. *Journal of Solid State Chemistry* **1971**, *3*, 490-500.
- (6) Zylbersztejn, A.; Mott, N. Metal-insulator transition in vanadium dioxide. *Physical Review B* **1975**, *11*, 4383-4395.
- (7) Booth, J.; Casey, P. Anisotropic Structure Deformation in the VO<sub>2</sub> Metal-Insulator Transition. *Physical Review Letters* **2009**, *103*, 086402-086406.
- (8) Wentzcovitch, R.; Schulz, W.; Allen, P. VO<sub>2</sub>: Peierls or Mott-Hubbard? A view from band theory. *Physical Review Letters* **1994**, *72*, 3389-3393.
- (9) Shi, J.; Bruinsma, R.; Bishop, A. Theory of vanadium dioxide. *Synthetic Metals* **1991**, *43*, 3527-3530.
- (10) Woodley, S. The mechanism of the displacive phase transition in vanadium dioxide. *Chemical Physics Letters* **2008**, *453*, 4-6.
- (11) Qazilbash, M.; Brehm, M.; Chae, B.; Ho, P.; Andreev, G.; Kim, B.; Yun, S.; Balatsky, A.; Maple, M.; Keilmann, F.; Kim, H.; Basov, D. Mott Transition in VO<sub>2</sub> Revealed by Infrared Spectroscopy and Nano-Imaging. *Science* **2007**, *318*, 21750-1753.
- (12) Guan, S.; Rougier, A.; Suchomel, M.; Penin, N.; Bodiang, K.; Gaudon, M. Geometric considerations of the monoclinic-rutile structural transition in VO<sub>2</sub>. *Dalton Transactions* **2019**, *48*, 9260-9265.
- (13) Dietrich, M. K.; Kuhl, F.; Polity, A.; Klar, P. J. Optimizing thermochromic VO<sub>2</sub> by co-doping with W and Sr for smart window applications. *Applied Physics Letters* **2017**, *110*, 141907-141912.
- (14) Krammer, A.; Bouvard, O.; Schüler, A. Study of Si doped VO<sub>2</sub> thin films for solar thermal applications. *Energy Procedia* **2017**, *122*, 745-750.
- (15) Amiche, A.; El Hassar, S. M. K.; Larabi, A.; Khan, Z. A.; Khan, Z.; Aguilar, F. J.; Quiles, P. V. Innovative overheating solution for solar thermal collector using a reflective surface included in the air gap. *Renewable Energy* **2020**, *151*, 355-365.
- (16) Peng, L. Y.; Wang, D.; Liang, J.; Hu, C.; Nishibori, E.; Sun, L.; Fisher, C. A. J.; Tanemura, S. Characterisation of the temperature-dependent M1 to R phase transition in W-doped VO<sub>2</sub> nanorod aggregates by Rietveld refinement and theoretical modelling. *Physical Chemistry Chemical Physics* **2020**, *22*, 7984-7994.
- (17) Zhang, R.; Jin, H. B.; Guo, D.; Zhang, J.; Zhao, Z.; Zhao, Y. The role of Fe dopants in phase stability and electric switching properties of Fe-doped VO<sub>2</sub>. *Ceramics International* **2016**, *42*, 18764-18770.
- (18) Wu, Y.; Fan, L.; Chen, S.; Chen, S.; Chen, F.; Zou, C.; Wu, Z. A novel route to realize controllable phases in an aluminum (Al<sup>3+</sup>)-doped VO<sub>2</sub> system and the metal-insulator transition modulation. *Materials Letters* **2014**, *127*, 44-47.
- (19) Jia, C.; Wu, Z.; Wu, X.; Wang, J.; Liu, X.; Gou, J.; Zhou, H.; Yao, W.; Jiang, Y. Terahertz transmittance and metal-insulator phase transition properties of M2 phase VO<sub>2</sub> films induced by Cr doping. *Applied Surface Science* **2018**, *455*, 622-628.
- (20) Burkhardt, W.; Christmann, T.; Meyer, B.; Niessner, W.; Schalch, D.; Scharmann, A. W- and F-doped VO<sub>2</sub> films studied by photoelectron spectrometry. *Thin Solid Films* **1999**, *345*, 229-235.
- (21) Tan, X.; Liu, W.; Long, R.; Zhang, X.; Yao, T.; Liu, Q.; Sun, Z.; Cao, Y.; Wei, S. Symmetry-Controlled Structural Phase Transition Temperature in Chromium-Doped Vanadium Dioxide. *The journal of physical chemistry* **2016**, *120*, 28163-28168.
- (22) Wieser, E.; Brückner, W.; Thuss, B.; Gerlach, U. Mössbauer effect studies on modified VO<sub>2</sub>. V<sub>1-x</sub>Fe<sub>x</sub>O<sub>2-y</sub> and V<sub>1-x-z</sub>Fe<sub>x</sub>Mo<sub>z</sub>O<sub>2</sub>. *Physica Status Solidi A* **1978**, *45*, 123-131.
- (23) Kosuge, K.; Kachi, S. Phase diagram of Fe<sub>x</sub>V<sub>1-x</sub>O<sub>2</sub> in the 0 ≤ x ≤ 0.25 region. *Materials Research Bulletin* **1976**, *11*, 255-262.
- (24) Zhang, Y.; Zhang, J.; Zhang, X.; Huang, C.; Zhong, Y.; Deng, Y. The additives W, Mo, Sn and Fe for promoting the formation of VO<sub>2</sub>(M) and its optical switching properties. *Materials Letters* **2013**, *92*, 61-64.
- (25) Phillips, T.; Murphy, R.; Poehler, T. Electrical studies of reactively sputtered Fe doped VO<sub>2</sub> thin films. *Materials Research Bulletin* **1987**, *22*, 1113-1123.
- (26) Rajpure, K. Y. Exploring structural and magnetic properties of nanocrystalline iron oxide synthesized by autocombustion method. *Superlattices and Microstructures* **2015**, *77*, 181-195.
- (27) Krammer, A.; Magrez, A.; Vitale, W. A.; Mocny, P.; Jeanneret, P.; Guibert, E.; Whitlow, H. J.; Ionescu, A.; Schüler, A. Elevated transition temperature in Ge doped VO<sub>2</sub> thin films. *Journal of Applied Physics* **2017**, *122*, 045304-045310.
- (28) Wang, X.; Rogalla, D.; Kostka, A.; Ludwig, A. Influence of low Bi contents on phase transformation properties of VO<sub>2</sub> studied in a VO<sub>2</sub>:Bi thin film library. *RSC Advances* **2021**, *11*, 7231-7237.

# TOC Graphic

